094046

(7)

Published online June 13, 2005

Vadose Zone Clays and Water Content beneath Wet and Dry Canyons of the Pajarito Plateau, New Mexico

D. Vaniman,* D. Broxton, and S. Chipera

ABSTRACT

Clay mineralogy in the vadose zone at Los Alamos National Laboratory (LANL), situated on the Pajarito Plateau of northern New Mexico, differs significantly beneath wet and dry canyons. Drainage across LANL is generally from west to east and feeds into the Rio Grande along the eastern margin of the plateau. Canyons with headwaters in the Sierra de los Valles west of the plateau support more flow and are wetter than canyons with headwaters on the plateau. Los Alamos Canyon, one of the wetter canyons, has extensive clay alteration to depths >30 m in the subcanyon vadose zone. Mortandad Canyon, one of the drier canyons, has less clay alteration. Hydraulic property data for the Otowi Member of the Bandelier Tuff, one of the most widespread lithologies of the plateau, indicate that zones of high clay abundance have hydraulic transmissivities (K_{sat}) one to two orders of magnitude lower than less altered tuff (~10^{-4} vs. 10^{-2} to 10^{-3} cm/s). Occurrences of halloysite, and perhaps kaolinite, indicate zones where the water/rock ratio is or has been high within the vadose zone. Gravimetric water content data collected at 110°C from vadose zone rocks with low to moderate clay content provide water abundance data for matrix flow calculations. These data may be in error by up to ~5 to 16% because some of the water measured is actually held in clay interlayers rather than in pore spaces; such errors are minor but should be considered in the use of gravimetric moisture data. The use of electrical methods to explore for vadose wet zones is valid on the Pajarito Plateau as long as the results are treated broadly, with the understanding that some intervals of high conductivity are not entirely related to either movable water content or clay abundance.

THE FACILITIES of Los Alamos National Laboratory (LANL) are located in northern New Mexico on mesa tops and within canyons of the Pajarito Plateau, a gently east-sloping surface that is bounded on the east by the Rio Grande in White Rock Canyon (Fig. 1). The portion of the Pajarito Plateau where LANL facilities are located is underlain by deposits of Bandelier Tuff, a sequence of siliceous pyroclastic deposits erupted in two major episodes at 1.61 and 1.22 Ma (Izett and Obradovich, 1994). These deposits have been eroded into a series of finger mesas by canyons that allow access to deep exposures, particularly of the 1.22 Ma Tshirege Member that has been most incised by erosion. The deepest canyons cut through a varied sequence of sediments and tuffs of the Cerro Toledo interval (1.22–1.61 Ma) and into the Otowi Member of the Bandelier Tuff (1.61. Ma). In some eastern canyon reaches, streams have cut into underlying volcaniclastic sediments of the Puye Formation and Cerros del Rio basaltic lavas. Descriptions of these stratigraphic units are provided in a companion paper in this volume (Broxton and Vaniman, 2005).

The facilities of LANL, including waste storage and disposal areas, are located primarily on mesa tops, but discharges of treated wastewater have occurred in several of the canyons. The focus of this study is on two canyons (Fig. 1): Los Alamos Canyon, which has headwaters in the Sierra de los Valles dacitic volcanic terrain to the west of LANL and Mortandad Canyon, with headwaters in Bandelier Tuff deposits of the Pajarito Plateau. Flow in these two canyons is fundamentally different (Purtymun, 1995), for the amount of rainfall and snowmelt in the drainage area of Los Alamos Canyon [29 km² (10.6 mi²) extending to 3170 m (10 400 ft) elevation] far exceeds the abundance of precipitation that feeds flow in Mortandad Canyon [drainage area of 5 km² (1.8 mi²) extending to 2290 m (7500 ft) elevation]. Flow in Los Alamos Canyon is sufficient to reach the Rio Grande in many rainfall events and as snowmelt occurs. Flow in Mortandad Canyon is seasonal and only extends to the Rio Grande under exceptional flood conditions. However, discharges of LANL effluents into Mortandad Canyon maintain perennial pulses of flow in the upper and midreaches (west of MCOBT-4.4; see Fig. 1).

Clay Mineralogy: Smectite, Illite, Kaolinite, Halloysite

The mineralogic focus of this study is on clays. Other authigenic minerals occur in the canyon systems at LANL, but these are relatively minor components found in a few occurrences and with limited distribution (zeolites, calcite, gypsum, and halite) or they are components with widespread distribution (Mn, Fe oxyhydroxides) that are yet poorly characterized. All of these other authigenic minerals are generally present in only trace amounts (<1%, w/w), whereas clays can occur in some portions of the canyon systems in abundances up to ~50% (w/w) or more.

Clay minerals common to the LANL canyon systems include both clays of the 2:1 structural series (clays having a tetrahedral sheet on both sides of an octahedral sheet) and clays with 1:1 structures (clays having a tetrahedral sheet on only one side of an octahedral sheet). The 2:1 clays of the canyons are principally smectites, with lesser amounts of illite; the 1:1 clays of the canyons include kaolinite and halloysite.

Smectites are swelling clays; that is, clays that have hydrated cations (typically Na, Ca, and lesser K) between the 2:1 layers and capable of gaining water in this interlayer zone, expanding the clay structure (Bailey, 1984). These cations provide a positive charge that compensates for a negative "layer charge"

D. Vaniman, MS D462, Los Alamos National Lab., Los Alamos, NM 87545; D. Broxton, MS T003, Los Alamos National Lab., Los Alamos, NM 87545; and S. Chipera, MS D469, Los Alamos National Lab., Los Alamos, NM 87545. Received 27 Apr. 2004. *Corresponding author (vaniman@lanl.gov).

Published in Vadose Zone Journal 4:453–465 (2005).
Special Section: Los Alamos National Laboratory
doi:10.2136/vzj2004.0068
© Soil Science Society of America
677 S. Segoe Rd., Madison, WI 53711 USA

Abbreviations: LANL, Los Alamos National Laboratory; QXRD, quantitative powder X-ray diffraction.

Science Society of America. All copyrights reserved.

14495

(H)

Best Available Copy

Reproduced from Vadose Zone Journal. Published by Soil Science Society of America. All copyrights reserved.

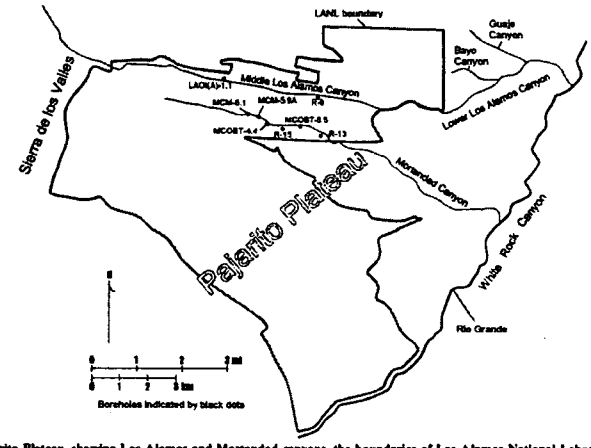

Fig. 1. The Pajarito Plateau, showing Los Alamos and Mortandad canyons, the boundaries of Los Alamos National Laboratory (LANL), and the boreholes discussed in this paper (labeled dots).

generated largely by the substitution of Al for Si in the tetrahedral sites. Illites are K-rich equivalents that have essentially lost the capability to expand because of a strong layer charge that stabilizes the high K content. These two types of clay are very similar in structure and often occur interstratified (high-K illite structures interlayered with expandable smectite structures). In both illites and smectites "water" occurs as OH at octahedral apices that are not shared with tetrahedra. Unlike smectites, illites have little or no H_2O in the interlayers between 2:1 sheet structures.

Kaolinites and halloysites are not swelling clays; these 1:1 structures do not have hydrated cations in their interlayers, although halloysite generally has some water of hydration between the 1:1 layers (Churchman et al., 1972; Brindley, 1984). In kaolinite the oxygen atoms in the outer face of one tetrahedral sheet are linked to hydroxyls in the outer portion of the octahedral sheet in the next 1:1 layer by H bonds, providing a relatively rigid, platy structure. In halloysite the H bonds linking 1:1 sheets are misaligned, causing the 1:1 layers to curl into cylindrical shapes (e.g., Levis and Deasy, 2002).

The abundance of 1:1 clays in the canyons is distinctive from clay assemblages of the surrounding mesas, where clays of the soils and in the Bandelier Tuff are dominantly smectites with interstratified illite and very minor amounts of kaolinite (Vaniman et al., 2002). To date halloysite has not been found in the mesa environment.

Many of the samples discussed here contain hydrated volcanic glasses, which typically lose ~2 to 4% (w/w) water on heating to temperatures >200°C (Vaniman et al., 1993). Any contribution of water from volcanic glasses will be negligible at the temperature used for gravimetric water determination (110°C), as discussed in this paper.

MATERIALS AND METHODS

Petrographic analyses were conducted using standard polished thin sections and an Olympus BH-2 petrographic microscope. Mineral abundances in drill core samples were determined by quantitative powder X-ray diffraction (QXRD) with a Siemens D-500 diffractometer using Cu-Kα radiation and a Kevex Psi Si(Li) solid state detector. Data were obtained on samples that were first crushed in a tungsten-carbide shatterbox and then ground to <5 μm in an automatic agate Brinkman Micro-Rapid mill. For data collected from drill hole LAOI(A)-1.1, a portion of each sample was mixed with a 1.0-μm corundum internal standard in a sample/corundum ratio of 4:1 by weight. The quantitative mineralogy was determined on a weight basis using the methods outlined by Chung (1974). Glass was determined by difference after the abundances of crystalline phases were determined; for this reason the totals in such analyses are always 100%. These QXRD methods have been coded into a computer program (QUANT) that accounts for analytical problems important in the analysis of tuffs, altered tuffs, and soils: for example, correction of clinoptilolite and opal-CT for mutual overlap and use of multiple reflections to improve results for analysis of complex tectosilicates. Further details of the basic method can be found in Bish and Chipera (1988, 1989) and the methods of multireflection analysis are described in Chipera and Bish (1995). For all other QXRD analyses, collected at a later date, the same diffraction instrument was used but quantitative analysis was performed with a full-pattern quantitative analysis program (FULLPAT) using measured and calculated patterns (Chipera and Bish, 2002). All phases including glass are modeled and totals are not constrained to 100%. In this more recent method it is possible to distinguish between kaolinite and halloysite; in the older data for LAOI(A)-1.1 these two clays are not differentiated and are listed as "kaolinite/halloysite."

In all boreholes, core samples were collected for water content analysis and analysis of soluble-ion leachates using deionized water. Each core sample was sealed in a pre-weighed container at the drill site to prevent moisture loss before anal-

RECEIVED
OCT 24 2006
By

Reproduced from Vadose Zone Journal. Published by Soil Science Society of America. All copyrights reserved.

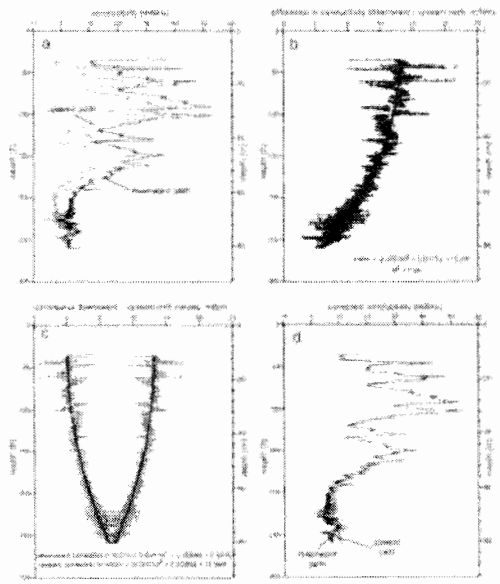

Fig. 2. Raw and corrected conductivity logs from borehole B-9. The instrument was calibrated before the logging run. Slightly different to signal with time in case of malfunction, of data. Note, downward and upward instrument paths (arrows). The gain of the raw signal is systematically and due to, for [illegible] a set conductivity structure of [illegible] slightly to [illegible] with [illegible] of 0.94. The correction function can be applied to the signal taken at each depth in both downward and upward paths (arrows) to generate corrected values that account for instrument drift (Fig. 3b).

Reproduced from Vadose Zone Journal. Published by Soil Science Society of America. All copyrights reserved.

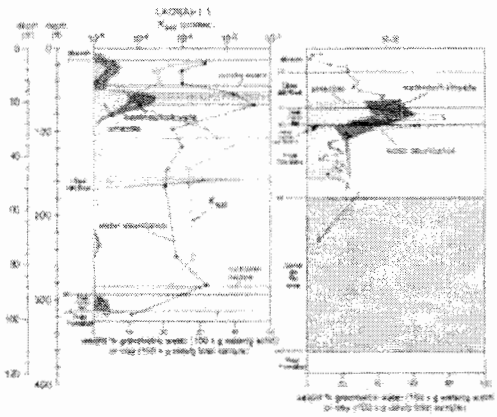

Fig. 3. Synoptic water attendance profiles and slug attenuations in drill holes LAGEN-A-1.1 and B-9 middle East Alabama Campus. Note that the lower horizontal scales, for weight to water and slug, differ for the two drill holes (B-9 is modern) and also that for B-9 cover a greater footwall depth range than the moderate data. The figure for LAGEN-A-1.1 also shows hydraulic conductivity data (K$_{sat}$) from Kerfoot et al. (1995). Fluctuations in the figure for LAGEN-A-1.1 indicate semi-vertical dip-filled fracture zones while soaklings indicate a gradual swaying and a horizontal fracture zone at seafloor.

Except to achieve an overall fit to [illegible] the conceptually that the [illegible] were [illegible] that [illegible] of the [illegible] to the [illegible] [illegible] the [illegible] that the additional [illegible] [illegible] of [illegible] its [illegible] and the [illegible] of [illegible] was [illegible] [illegible] [illegible]

Reproduced from Vadose Zone Journal. Published by Soil Science Society of America. All copyrights reserved.

Table 2. Quantitative XRD data for the vadose zone in Drill Hole R-8 (%, w/w).†

Stratum‡	Depth	Smectite	Illite	Halloysite	Kaolinite§	Clinoptilolite	Tridymite	Cristobalite	Quartz	K feldspar	Plagioclase	Glass	Hematite	Biotite	Hornblende	Total
	m															
Qbo	19.6	24.0	8.8	20.0	–	–	–	–	10.9	5.2	14.5	14.1	0.3	0.1	–	97.0
Qbog	25.0	26.7	11.2	24.2	–	–	–	–	9.8	3.6	4.4	22.4	0.1	–	–	102.5
Tpf-p	29.0	7.1	8.9	23.8	–	–	–	0.8	1.4	0.9	18.9	33.4	0.1	–	–	95.4
Tpf	34.0	14.3	7.6	2.0	–	1.1	5.0	6.6	13.3	11.4	27.6	18.0	0.7	1.5	0.4	101.6
Tpf	48.1	17.3	6.7	–	0.9	1.2	4.1	5.5	15.1	8.7	31.2	5.8	0.6	1.6	0.3	99.0
Tpf	135.5	0.1	1.2	–	1.2	–	9.8	6.6	0.1	12.1	40.4	22.3	0.5	1.6	0.2	96.3
Tpf	176.6	7.1	2.0	–	0.2	–	3.6	4.7	21.6	17.3	38.8	–	0.7	3.4	0.2	99.7

† Dashes = nondetection.
‡ Strata include ash flows of the Otowi Member of the Bandelier Tuff (Qbo), the Guaje Pumice Bed at the base of the Otowi Member (Qbog), a dacitic pumice bed at the top of the Puye Formation (Tpf-p), and fanglomerates of the Puye Formation (Tpf).
§ May include some halloysite.

data were obtained than for LAOI(A)-1.1, but the data from R-8 are sufficient to show that clay abundances are considerably greater in the Otowi ash flows and the Guaje Pumice Bed at R-8 than in these units in LAOI(A)-1.1 (50-60%, vs. <20% in all but one of the LAOI(A)-1.1 Otowi ash flow and Guaje Pumice Bed samples). This greater abundance of clays in R-8 is distributed throughout the matrix and is not closely linked to occurrences of fracture zones, as is the case in the Otowi ash flows at LAOI(A)-1.1.

In drill holes MCOBT-4.4 and MCOBT-8.5 the bulk core samples are relatively unaltered (Table 3). The small amount of alteration observed in the core samples is predominantly smectite (0–2.7%, w/w) with kaolinite occurring only in Cerro Toledo ash at 20.7 to 20.8 m (68.0–68.2 ft) depth in MCOBT-4.4. In contrast, mineralogic data obtained for particulates leached from lightly crushed core indicate a predominance of clays (Table 4), with smectite most common in drier portions of the sequence and halloysite (± illite) more common in wetter portions of the water abundance profiles. On evaporation of leachates halite, calcite, and possibly gypsum salts were produced from some samples. The mineralogy of the <50 nm clay and salt fractions is annotated on Fig. 4 against the water abundance profiles in these drill holes.

Water Abundance Data, Electrical Conductivity Data, and Mineralogy

The water abundance profile in drill hole R-8 is shown in Fig. 5, with points on the water abundance curve to indicate locations of core samples analyzed. These gravimetric water content data are plotted along with drift-corrected conductivity data collected in R-8 using the Mount Sopris induction probe. In a very broad sense the region of highest conductivity from about 15.2 to 33.5 m (50–110 ft) depth corresponds with core samples of highest water content. In detail the correlation between conductivity and water content shows several points of deviation from the local trend of increasing or decreasing water content (circled data points in Fig. 5).

A bivariate plot of water abundance and conductivity data from R-8 is shown in Fig. 6, with conductivities representing induction probe data from the same depth as each analyzed core sample. Many samples, regardless of lithology, can be interpreted to fit a regression that excludes the circled outliers in Fig. 6; in this regression the adjusted water content, represented as % (w/w) water abundance ÷ total sample mass, is approximately 0.9 times the local value of conductivity in mS/m. The samples that deviate most from this relationship diverge because they are more conductive than their water content would otherwise indicate.

Core Hydrogeologic Properties in LAOI(A)-1.1

The hydrogeologic properties of core samples from borehole LAOI(A)-1.1 are summarized in Table 5. Results are tabulated for ASTM water abundance values (g water/g dry mass), dry bulk density, calculated porosity, and hydraulic transmissivity. The hydraulic transmis-

Reproduced from Vadose Zone Journal. Published by Soil Science Society of America. All copyrights reserved.

Table 3. Quantitative XRD data for the vadose zone in Drill Holes MCOBT-4.4 and MCOBT-8.5 (%, w/w).†

Stratum‡	Depth	Smectite	Kaolinite§	Tridymite	Cristobalite	Quartz	K feldspar	Plagioclase	Glass	Hematite	Biotite	Hornblende	Total
	m												
						MCOBT-4.4							
Qct	20.8	–	1.1	–	–	0.3	1.0	–	95.1	–	–	–	98.5
Qct	24.2	0.1	–	0.7	0.8	5.3	4.4	8.8	77.8	–	–	0.3	98.2
Qct	25.9	1.7	–	1.6	1.1	9.2	9.8	17.8	57.3	0.1	–	0.3	98.9
						MCOBT-8.5							
Qal/Qc	17.5	2.7	–	8.1	–	33.5	20.0	26.6	4.9	0.5	0.1	–	96.4
Qal/Qc	32.7	–	–	2.8	0.9	13.5	8.8	20.1	54.3	0.5	–	0.1	100.2

† Dashes = nondetection.
‡ Strata include alluvium/colluvium (Qal/Qc) and sediments of the Cerro Toledo Interval (Qct).
§ Kaolinite in MCOBT-4.4 at 20.8 m depth may include some halloysite.

sivity and water abundance data are plotted against tratigraphy, fracture zones, and clay mineralogy in Fig. 3. The lowest hydraulic transmissivities ($<10^{-4}$ cm/s) for the Otowi ash flows occur in clay-rich fracture zones. The highest transmissivity ($\sim10^{-2}$ cm/s) occurs within a sample of unaltered ash flow at 36.1 m (118.5–118.6 ft) depth. The single sample analyzed from the Puye fanglomerate has higher hydraulic transmissivity than all of the Otowi samples except this most transmissive sample from the Otowi ash flows.

DISCUSSION

Clay Distributions and Pathways for Flow

The data from LAOI(A)-1.1 show that fracture zones (Fig. 3) can have a significant role in defining the distribution of clays in the vadose zone. Total clay abundance reaches 40% (w/w) of smectite plus kaolinite/halloysite in some fracture zones, but the matrix alteration outside the fracture zones is generally limited to <3% (w/w) of mainly smectite. Petrographic data from the fracture zones in the Otowi ash flows consistently indicate a trend of early smectite formation followed by later kaolinite/halloysite fracture filling. The hydrologic properties data from this drill hole (Table 5 and Fig. 3) show that the permeability of clay-filled fractures in Otowi ash flows is one to two orders of magnitude less than the permeability of the unaltered tuff matrix. This observation, plus the evidence that (i) matrix alteration of the ash flows is limited to smectite and (ii) kaolinite/halloysite is limited to fracture zones or perched horizons (alluvium and Guaje Pumice Bed), favors an interpretation of late-stage introduction of kaolinite/halloysite into previously smectite-filled fractures that have been reopened, possibly by tectonic events.

Within Los Alamos Canyon, differences in clay abundance and distribution between LAOI(A)-1.1 and R-8 are striking. In R-8 (Fig. 3) there is a high abundance of both smectite and halloysite, with total clay abundances of 40 to 60% (w/w) in three samples representing the Otowi ash flows, the Guaje Pumice Bed, and an older dacitic pumice unit just below the Guaje Pumice Bed at 29 m (95 ft) depth. Examination of cores suggests that such clay abundances are pervasive in the tuff units above the Puye Formation at R-8. The implication of the R-8 data is that high gravimetric water content and extensive alteration extend down to ~30 m (~100 ft) depth in this portion of Los Alamos Canyon by matrix communication without localization in fracture systems. At present there are insufficient data to determine how much of the clay is formed in place and how much is translocated. In contrast to LAOI(A)-1.1, clay accumulations in R-8 are not focused along fracture zones, suggesting that pervasive saturation led to extensive clay formation in place beneath this portion of Los Alamos Canyon.

The data from drill holes MCOBT-4.4 and MCOBT-8.5 in Mortandad Canyon indicate that smectite and halloysite are common in the leachates from core samples (Table 4), although small amounts of illite also occur. When the <50 nm leachate mineralogy is plotted along with the water abundance curves for these drill holes (Fig. 4) the distribution of smectite vs. halloysite suggests that the halloysite tends to be correlated with zones of higher gravimetric water content. This conclusion is supported by the clay distributions plotted in Fig. 3, where the two zones of perched saturation in LAOI(A)-1.1, within alluvium and within the Guaje Pumice Bed, have clay assemblages dominated by kaolinite/halloysite with smectite less common.

The data from both Los Alamos Canyon and Mortandad Canyon support a correlation between higher gravimetric water content and kaolinite/halloysite occurrences in the vadose zone. The petrographic evidence for early smectite formation and later kaolinite/halloysite formation in Los Alamos Canyon may indicate a transition over time in the nature of clay formation within the canyons of the Pajarito Plateau. However, the cause of this shift from 2:1 to 1:1 clays over time is not clear. Contributing factors may be differences in access to vadose zone flow, progressive modification of groundwater composition, effects of changing water/rock ratio in determining the nature of clay alteration, and in some instances variation in relative contributions from authigenic clay formation vs. translocation.

Water Residence in Pores and in Clays

The combination of quantitative water abundance data with quantitative determination of clay types and abundances allows an estimation of how much vadose zone water is held within minerals compared with the water in pore spaces. Such an analysis for five samples from drill hole R-8 is provided in Table 6. The corre-

Reproduced from Vadose Zone Journal. Published by Soil Science Society of America. All copyrights reserved.

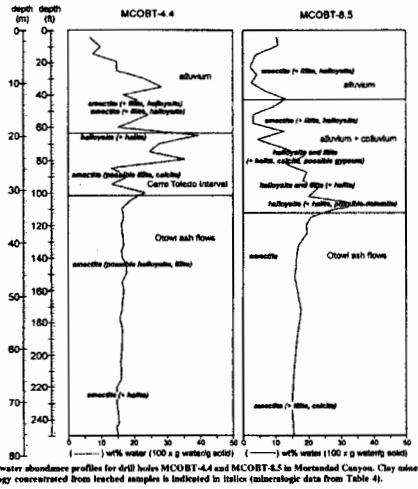

Fig. 4. Gravimetric water abundance profiles for drill holes MCOBT-4.4 and MCOBT-8.5 in Mortandad Canyon. Clay mineralogy of particulates and salt mineralogy concentrated from leached samples is indicated in italics (mineralogic data from Table 4).

clays are not intimately intergrown, kaolinite (possibly including halloysite) is differentiated from smectite by lower birefringence (first-order birefringence, <0.001 in kaolinite, vs. second-order birefringence, 0.003–0.004, in smectite). The samples analyzed represent both altered matrix and clay-filled fractures.

A thin section prepared from a vertical fracture zone high in the Otowi ash flows (16.5–16.8 m, or 54.2–55.0 ft depth) has vertical fracture-filling stringers of coarse kaolinite and smectite. Kaolinite is generally concentrated along the fracture axes, with smectite lining the fracture walls and penetrating the matrix near the fractures. Pumice lapilli in the matrix of this sample exclude clay, but some pumice along the fractures are clay-filled. Clays within the fractures have small-scale (~200 μm) chevron structure, suggesting either clay expansion within fracture confinement or fracture slippage after clay formation.

At somewhat greater depth in the Otowi ash flows (18.7–18.9 m, or 61.5–61.9 ft), fractures are irregular and form a boxwork texture that fragments many pumice lapilli. Porous pumice lapilli that are not fractured are generally not invaded by clay. The clays drape both pumice and phenocrysts.

In a near-vertical clay seam deeper in the Otowi ash flows at 47.5 to 48.8 m (156–160 ft) depth, a thin section from a sample at 48.3 m (158.5 ft) depth shows elongate bodies of kaolinite (~0.1–0.5 mm wide) encased within smectite; in reflected light thin stringers of kaolinite (lower reflectivity) can be seen to penetrate between and across layers in the enclosing smectite, suggesting that kaolinite may have been introduced along small fractures that developed either when the smectite dehydrated and contracted or, more likely, when the fracture opened tectonically.

A sample from the upper part of the Puye Formation, at 97.4 m (319.5 ft) depth, is a moderately sorted clay-rich silty sand. Detrital grains are <100 μm in size and consist mostly of plagioclase, but include quartz, biotite, dacitic lithic fragments, and vitric pumice. Clays are dispersed throughout the porous matrix, and appear to be predominantly or entirely smectite; the vitric pumice has little or no clay alteration. Also dispersed throughout the matrix are small (~20–30 μm) opaque oxide bodies, possibly amorphous Mn- or Fe-oxyhydroxides.

Table 1. Quantitative XRD data for the vadose zone in Drill Hole LAOI(A)-1.1 (%, w/w).†

Stratum‡	Depth	Smectite	Kaolinite/halloysite	Tridymite	Cristobalite	Quartz	Feldspar	Glass	Hematite	Biotite	Total
	m										
Qal	2.2	tr	1	14	9	10	59	6	1	tr	100
Qbo	5.2	–	6	3	1	11	29	50	tr	–	100
Qbo	7.7	4	4	3	2	11	31	45	–	tr	100
Qbo	12.1	–	4	1	2	10	32	51	–	–	100
Qbo	15.6	–	3	1	2	11	21	62	–	–	100
Qbo	16.5	9	6	1	1	9	26	48	–	–	100
Qbo	18.7	10	8	1	1	15	32	33	–	–	100
Qbo	21.1	9	7	2	2	20	36	24	tr	–	100
Qbo	26.0	2	1	5	2	10	32	48	tr	–	100
Qbo	29.4	–	–	1	3	11	28	56	1	–	100
Qbo	32.3	2	–	1	3	11	27	56	–	–	100
Qbo	39.1	2	–	tr	3	10	26	59	–	–	100
Qbo	43.2	tr	–	1	2	13	25	59	–	–	100
Qbo	46.7	tr	–	2	4	11	27	56	–	–	100
Qbo	48.3	32	9	–	1	4	10	44	–	–	100
Qbo	52.7	tr	–	1	2	16	25	56	tr	tr	100
Qbo	57.5	1	–	–	2	11	25	61	tr	–	100
Qbo	62.4	–	–	–	2	11	23	64	–	–	100
Qbo	66.8	tr	–	–	2	10	27	61	–	–	100
Qbo	71.4	1	1	–	2	12	25	58	1	–	100
Qbo	76.1	tr	–	–	2	10	24	64	–	–	100
Qbo	81.4	tr	–	–	–	7	16	77	–	–	100
Qbo	89.0	tr	–	–	1	12	26	61	–	–	100
Qbog	92.1	tr	4	–	–	9	15	72	–	tr	100
Qbog	96.0	–	5	–	–	5	15	75	–	–	100
Qbog	96.3	7	3	2	4	20	34	29	tr	1	100
Tpf	96.7	2	1	9	12	6	55	13	1	1	100
Tpf	97.6	5	–	8	11	12	49	12	2	1	100

† Dashes = nondetection; tr = indicates trace abundance (< 0.5%, w/w).
‡ Strata include alluvium (Qal), ash flows of the Otowi Member of the Bandelier Tuff (Qbo), the Guaje Pumice Bed at the base of the Otowi Member (Qbog), and fanglomerates of the Puye Formation (Tpf).

This petrographic survey of a few representative thin sections from clay-rich zones of LAOI(A)-1.1 provides evidence that kaolinite (possibly including halloysite) has in many cases formed after the principal smectite alteration, either within the axial zones of small fractures lined by earlier smectite or in basal or cross-breaking fractures that disrupt preexisting smectite bodies.

Water Abundance Profiles and Clay Mineralogy

Gravimetric water abundance profiles and clay mineral abundances in two drill holes in Los Alamos Canyon, LAOI(A)-1.1 and R-8, are compared in Fig. 3. Water abundance data and leached particulate or salt mineralogy data for drill holes in Mortandad Canyon, MCOBT-4.4 and MCOBT-8.5, are provided in Fig. 4. In all drill holes except MCOBT-8.5 there is a prominent peak in water content at depths between 18.3 and 24.4 m (60 and 80 ft); in MCOBT-8.5 the peak water content is deeper (32.0 m, or 105 ft depth). Water abundance profile data are also available from other drill holes in Mortandad Canyon: R-15, MCM-5.1, and MCM-5.9a (drill hole locations shown in Fig. 1). In these drill holes, the peak water content is also reached at depths between 18.3 and 36.6 m (60 and 120 ft) (Longmire et al., 2001). In most cases the maximum in water content occurs within alluvium/colluvium or in underlying sediments of the Cerro Toledo Interval.

Mineralogic analysis by XRD includes both quantitative (QXRD) and semi-quantitative analyses. The QXRD results for drill hole LAOI(A)-1.1, collected using the methods of Chipera and Bish (1995), are listed in Table 1. The QXRD results for drill holes R-8, MCOBT-4.4, and MCOBT-8.5 collected using more recent methods (Chipera and Bish, 2002), are listed in Tables 2 and 3. Semi-quantitative XRD data for leachate samples of settled (50–200 nm) and suspended (<50 nm) solids obtained from leachate samples of MCOBT-4.4 and MCOBT-8.5 are listed in Table 4. These data show highly variable abundances and distributions of clay minerals in the vadose zone beneath Los Alamos and Mortandad canyons. There are nevertheless some systematic aspects to clay occurrences dependent on depth, presence or absence of fracture zones, and in particular whether the canyon is relatively wet or dry.

In drill hole LAOI(A)-1.1, mineralogic data were obtained from core samples representing alluvium, the Otowi ash flows, the Guaje Pumice Bed, and the Puye Formation (Table 1); most of the data are from the Otowi ash flows. In this drill hole there is an abundance of kaolinite/halloysite as well as smectite to a depth of 21.3 m (70 ft). Below this depth kaolinite/halloysite does not occur in the Otowi ash flows, except in a clay-filled fracture at 48.3 m (158.5 ft) depth and in minor amount at a depth of 71.4 m (234.1 ft). Kaolinite reappears in abundances of 3 to 5% (w/w) in the Guaje Pumice Bed (89.6–96.3 m, or 294–316 ft depth). During drilling, zones of local saturation within the vadose zone were observed at the base of the alluvium (2.4–4.6 m, or 8–15 ft depth) and within the Guaje Pumice Bed (89.6–96.3 m, or 294–16 ft depth; Newell, 1994).

In drill hole R-8, mineralogic data were obtained from core samples representing the Otowi ash flows, the Guaje Pumice Bed, and the Puye Formation (Table 2). Fewer

Reproduced from Vadose Zone Journal. Published by Soil Science Society of America. All copyrights reserved.

Reproduced from Vadose Zone Journal. Published by Soil Science Society of America. All copyrights reserved.

Reproduced from Vadose Zone Journal. Published by Soil Science Society of America. All copyrights reserved.

specific demonstration of high bulk conductivity and included for comparison with Fig. 3. In Table 6 we show the additional water contents of the samples (lower in 18 m and at 1783.2) relative to pore fluids types of samples and third. When a sample is heated to 110°C in the ASTM water abundance determination procedure, water will be lost and with but not all clay water will be retained.

Within the first clay mineral layer adjacent silica, hydrogen and hydroxyl the amount of water retained at 110°C depends in part on the clay composition (Fig. 10). Hence clayey or silty rocks, but the water difference is in response with the between dry or pore types of clay. Bound structural water within the soil by heat at 110°C, having potentially produced gypsum in the clay structure (Hall and Hall, 1989). For gypsum (type of SILTBELT rock) content is 15% (water and bound content 5%, water). For Nolanville (typical rock) clay rock content is 5% (water and bound content 14%, water). Bitter (5%, water) and Pedernal (water 14%, water). Bitter (5%, water) and Pedernal (water 14%, water). Approximately have comparable the relative water and their conductivity on water at 110°C. Clay phase values the amount of water contributed by clays on heating to 110°C, can be calculated for each sample (column 11 in Table 6), which can be subtracted from the total water

Reproduced from Vadose Zone Journal. Published by Soil Science Society of America. All copyrights reserved.

Table 5. Hydrologic Properties of Samples from Drill Hole LAOI(A)-1.1 (Stephens et al., 1995).

Stratum†	Depth	Water abundance (gravimetric)	Dry bulk density	Calculated porosity	Hydraulic transmissivity (K_{sat})	Hydraulic transmissivity method‡
	m	100 × g water/g dry mass	g/cm³	%	cm/s	
Qbo	4.8	11.9	1.92	27.7	3.4×10^{-3}	CH
Qbo	4.9	37.9	1.05	60.4	1.3×10^{-3}	CH
Qbo	5.7	31.5	1.16	56.1	5.4×10^{-4}	CH
Qbo	8.6	24.9	0.98	62.9	2.4×10^{-4}	FH
Qbo	13.3	25.2	0.99	62.6	3.4×10^{-4}	CH
Qbo	17.7	39.3	1.20	54.8	7.2×10^{-3}	FH
Qbo	21.0	45.3	1.17	55.7	7.6×10^{-3}	FH
Qbo	29.7	22.3	1.24	53.3	3.5×10^{-3}	CH
Qbo	36.1	25.2	1.11	58.2	1.4×10^{-3}	CH
Qbo	44.4	20.7	1.05	60.2	1.4×10^{-3}	CH
Qbo	50.3	20.2	1.27	52.2	1.5×10^{-3}	CH
Qbo	76.1	23.4	1.08	59.2	1.8×10^{-3}	CH
Qbo	86.2	31.9	0.94	64.7	5.3×10^{-4}	CH
Tpf	96.9	11.1	1.96	26.1	6.3×10^{-3}	CH

† Strata include ash flows of the Otowi Member of the Bandelier Tuff (Qbo) and fanglomerate of the Puye Formation (Tpf).
‡ CH = constant head. FH = falling head.

conductivity data are useful for identifying zones of increased gravimetric water content. On a finer scale there are several samples that stand out in deviation; these are circled in blue in both Fig. 5 and Fig. 6. These samples are not restricted to any one unit, but can be found in the Otowi ash flows, the Guaje Pumice Bed, and the Puye fanglomerates, although the highest proportion of outliers occurs in the Puye fanglomerates.

Some of the variability in water content or conductivity within specific units, whether along the regression line in Fig. 6 or not, appears to be correlated with specific petrographic variants or stratigraphic subzones. For instance, in Fig. 6 the gravimetric water abundance of the petrographically distinct dacitic pumice bed at the top of the Puye Formation (high vesicular glass abundance vs. abundance of dense crystalline lava clasts) is greater than the water abundance in any of the pumice-poor Puye fanglomerates, although the pumice-poor fanglomerates include outliers of high conductivity that approach or exceed the conductivity of the dacitic pumice bed. Another example of variation possibly linked to a stratigraphic subzone is the basal sample from the Guaje Pumice Bed, which has high conductivity, similar to the other Guaje samples, but lower water content.

A more detailed study would be required to determine why each of the circled samples in Fig. 6 deviates from the trend otherwise seen, but it is notable that the most common deviation from correlation is in the direction of higher than expected conductivity for a given water content, not lower conductivity. The implication of this comparison is that conductivity measurements, either from the surface or from down-hole tools, will more easily overestimate than underestimate water abundance. Nevertheless, the deviations noted in R-8 occur in a relatively small subset of the samples analyzed from a variety of volcanic and sedimentary lithologies. The broad-scale use of electrical methods in exploration for vadose zone water remains valid on the Pajarito Plateau.

SUMMARY

A previous study of clays in soils and fractures of the mesa-top environment on the Pajarito Plateau shows that the typical clays of the mesa environment are eolian-derived smectites, accumulated in soils and transported into fractures, with minor illite, rare kaolinite, and no halloysite (Vaniman et al., 2002). In contrast the clay alteration in both wet and dry canyons is distinct in (i) higher ratios of 1:1 to 2:1 clay structural types, with local predominance of 1:1 clays, and (ii) appearance of halloysite as a common alteration product. Wet canyons are marked by more extensive clay formation, particularly in the widespread vitric portions of the Bandelier Tuff, Cerro Toledo Interval, and Puye Formation. The occurrence of abundant kaolinite and especially halloysite can be used to identify zones of prolonged high water/rock ratios; in Los Alamos Canyon these zones can be subdivided into (i) an upper interval of ~30 m (100 ft) that is continuous with and extends below alluvial saturation, (ii) vertical fracture zones that tend to fill with smectite but may reopen and fill with kaolinite or halloysite, and (iii) the Guaje Pumice Bed at depths up to ~90 m (~300 ft).

Zones of high clay abundance in the lower Bandelier Tuff have hydraulic transmissivities (K_{sat}) one to two orders of magnitude lower than the less altered tuff (~10^{-4} vs. 10^{-2} to 10^{-3} cm/s). Water-loss characteristics of vadose zone rocks with low to moderate clay content under the conditions of ASTM water abundance measurements can provide water abundance data for matrix flow calculations, but water contents so estimated may be in error by ~5 to 16% because some of the water measured is actually held in clay interlayers. These errors are not so large as to preclude the direct use of such water abundance measurements for flow calculations, but the determination of movable water will be more accurate if the mineralogy and quantity of clays present is determined and the extractable water in these clays is accounted for.

The data summarized in Fig. 6 show that caution should also be used in inferring moisture content from borehole conductivity data. Higher conductivity is observed in some horizons than might be estimated from gravimetric moisture data. This is particularly the case in the Puye Formation fanglomerates, where >25% of the conductivity measurements are higher than ex-

Reproduced from Vadose Zone Journal. Published by Soil Science Society of America. All copyrights reserved.

Table 6. Water Content, Electrical Properties, Mineralogy, and Apportioned Water Sites at Five Horizons in Drill Hole R-8.

1	2	3	4	5	6	7	8	9	10	11	12	13	14
Stratum†	Water abundance sample depth	Adjusted water	Conductivity	Resistivity	Mineralogy sample depth	Smectite	Illite	Halloysite	Kaolinite	Clay water lost	Nonclay water lost	Clay water retained	Fraction lost water not from clays
	m	% w/w, 100 × g water/g total	mS/m	ohm-m	m	% (w/w)							
Qbo	19.31	34.5	40.4	24.7	19.6	24.0	8.0	20.0	–	3.68	30.79	4.72	0.89
Qbog	24.00	43.2	35.3	28.3	25.0	26.7	11.2	24.2	–	4.17	39.05	5.73	0.90
Tpf-p	28.39	38.7	42.5	23.5	29.0	7.1	8.9	23.8	–	1.80	36.92	4.49	0.95
Tpf	34.79	11.0	21.2	47.2	34.0	14.3	7.6	2.0	–	1.80	9.24	1.68	0.84
Tpf	48.45	15.6	25.2	39.7	48.1	17.3	6.7	–	0.9	2.08	13.47	1.59	0.87

† Column 1 lists stratigraphic assignment for each sample (Qbo = Otowi ash flows, Qbog = Guaje Pumice Bed, Tpf-p = dacitic pumice bed at the top of the Puye Formation, Tpf = Puye fanglomerate); column 2 lists midrange depth for each 0.06-m (0.2 ft) sample used to collect water abundance data; column 3 = adjusted water abundance data represented as percentage, g water/g total sample; column 4 = borehole conductivity at depth closest to water abundance measurement, in mS/m; column 5 = borehole resistivity at depth closest to water abundance measurement, in ohm-m; column 6 = sample depths for mineralogy determination by QXRD; columns 7–10 = clay mineral content in % (w/w) hydrated clay/% (w/w) total sample; column 11 = calculated water loss from sample at 110°C associated with clay interlayers; column 12 = calculated water loss from sample at 110°C not associated with clay interlayers; column 13 = calculated amount of structural water retained in clays and not lost at 110°C; column 14 = calculated fraction of water measured by the ASTM method that is derived from rock pores and not from clay interlayers.

pected. Because the Puye fanglomerates are not exceptionally clay-rich (Fig. 3), it is unlikely that the higher conductivity in these samples is related to clay content. Other factors that can affect conductivity (particle properties, water salinity, lithology, etc.) appear to have influence. Although further study would be needed to determine the nature and magnitude of these factors, the overall gross correlation between conductivity and movable water content indicates that electrical methods are still useful in exploration for groundwater in both wet (clay-rich) and dry (clay-poor) canyons.

ACKNOWLEDGMENTS

This research was supported under the Hydrogeologic Workplan for Los Alamos National Laboratory. Review comments from Associate Editor B. Newman, W.S. Baldridge, and two anonymous reviewers helped greatly in refining and improving the manuscript.

REFERENCES

Bailey, S.W. 1984. Structures of layer silicates. p. 1–124. *In* G.W. Brindley and G. Brown (ed.) Crystal structures of clay minerals and their X-ray identification. Mineralogical Society, London, UK.

Bish, D.L., and S.J. Chipera. 1988. Problems and solutions in quantitative analysis of complex mixtures by X-ray powder diffraction. Adv. X-ray Anal. 31:295–308.

Bish, D.L., and S.J. Chipera. 1989. Revised mineralogic summary of Yucca Mountain, Nevada. Rep. LA-1149-MS. Los Alamos Natl. Lab., Los Alamos, NM.

Bish, D.L., and C.J. Duffy. 1990. Thermogravimetric analysis of minerals. *In* J.W. Stucki et al (ed.) Thermal analysis in clay science. The Clay Minerals Society Workshop Lectures. Vol. 3:96–157.

Brindley, G.W. 1984. Order-disorder in clay mineral structures. p. 125–195. *In* G.W. Brindley and G. Brown (ed.) Crystal structures of clay minerals and their X-ray identification. Mineralogical Society, London, UK.

Broxton, D., D. Vaniman, P. Longmire, B. Newman, W. Stone, A. Crowder, P. Schuh, R. Lawrence, E. Tow, M. Everett, R. Warren, N. Clayton, D. Counce, E. Kluk, and D. Bergfeld. 2002. Characterization well MCOBT-4.4 and borehole MCOBT-8.5 completion report. Rep. LA-13993-MS. Los Alamos Natl. Lab., Los Alamos, NM.

Broxton, D.E., and D.T. Vaniman. 2005. Geologic framework of a groundwater system on the margin of a rift basin, Pajarito Plateau, north-central New Mexico. Vadose Zone J. 4 (this issue).

Chipera, S.J., and D.L. Bish. 1995. Multireflection RIR and intensity normalizations for quantitative analyses: Applications to feldspars and zeolites. Powder Diffr. 10:47–55.

Chipera, S.J., and D.L. Bish. 2002. FULLPAT: A full-pattern analysis program for X-ray powder diffraction using measured and calculated patterns. J. Appl. Crystallogr. 35:744–749.

Chung, F.H. 1974. Quantitative determination of X-ray diffraction patterns of mixtures: I. Matrix-flushing method for quantitative multicomponent analysis. J. Appl. Crystallogr. 7:519–525.

Churchman, G.J., L.P. Aldridge, and R.M. Carr. 1972. The relationship between the hydrated and dehydrated states of an halloysite. Clays Clay Miner. 20:241–246.

Izett, G.A., and J.D. Obradovich. 1994. $^{40}Ar/^{39}Ar$ age constraints for the Jaramillo Normal Subchron and the Matuyama–Brunhes geomagnetic boundary. J. Geophys. Res. 99:2925–2934.

Levis, S.R., and P.B. Deasy. 2002. Characterization of halloysite for use as a microtubular drug delivery system. Int. J. Pharm. 243:125–134.

Longmire, P., D. Broxton, W. Stone, B. Newman, R. Gilkeson, J. Marin, D. Vaniman, D. Counce, D. Rogers, R. Hull, S. McLin, and R. Warren. 2001. Characterization well R-15 completion report. Rep. LA-13749-MS. Los Alamos Nat. Lab., Los Alamos, NM.

Newell, D. 1994. Core sample log for drill hole LAOI(A)-1.1. *In* Draft Field Summary Report of RCRA Facility Investigation Baseline Characterization 1994 Activities, Operable Unit 1098. Technical

Reproduced from Vadose Zone Journal. Published by Soil Science Society of America. All copyrights reserved.

Areas 2 and 41 (March 1995 release). Appendix A-4. Los Alamos National Lab, Los Alamos, NM.

Purtymun, W.D. 1995. Geologic and hydrologic records of observation wells, test holes, test wells, supply wells, springs, and surface water stations in the Los Alamos area. Rep. LA-12883-MS. Los Alamos Natl. Lab., Los Alamos, NM.

Stephens, D.B., et al. 1995. Laboratory analysis of soil hydraulic properties of TA-2 soil samples. Daniel B. Stephens and Associates, Albuquerque, NM, prepared for ERM/Golder, Los Alamos, NM.

Vaniman, D., D. Bish, and S. Chipera. 1993. Dehydration and rehydration of a tuff vitrophyre. J. Geophys. Res. 98:22,309–22,320.

Vaniman, D.T., S.J. Chipera, D.L. Bish, M.C. Duff, and D.B. Hunter. 2002. Crystal chemistry of clay–Mn oxide associations in soils, fractures, and matrix of the Bandelier Tuff, Pajarito Mesa, New Mexico. Geochim. Cosmochim. Acta 66:1369–1374.

Washington Group International. 2003. Characterization well R-8 completion report. GPP-03-021. Washington Group Int., Los Alamos, NM.